Technische Universität Chemnitz

Sonderforschungsbereich 393

Numerische Simulation auf massiv parallelen Rechnern

J. X. Zhong, U. Grimm, R. A. Römer, and M. Schreiber

Level-Spacing Distributions of Planar Quasiperiodic Tight-Binding Models

Preprint SFB393/97-21

Preprint-Reihe des Chemnitzer SFB 393

SFB393/97-21 October 1997

Author's addresses:

J. X. Zhong, Department of Physics, Xiangtan University, Xiangtan 411105, P. R. China

Uwe Grimm, Rudolf A. Römer and Michael Schreiber, Institut für Physik, Technische Universität Chemnitz, D-09107 Chemnitz

`http://www.tu-chemnitz.de/sfb393/`

Level-Spacing Distributions of Planar Quasiperiodic Tight-Binding Models

J. X. Zhong,[1,2] U. Grimm,[1] R. A. Römer,[1] and M. Schreiber [1]

[1] *Institut für Physik, Technische Universität Chemnitz, D-09107 Chemnitz, Germany*

[2] *Department of Physics, Xiangtan University, Xiangtan 411105, P. R. China*

($Revision$: 2.5, printed April 7, 1998)

Abstract

We study statistical properties of energy spectra of two-dimensional quasiperiodic tight-binding models. Taking into account the symmetries of models defined on various finite approximants of quasiperiodic tilings, we find that the underlying universal level-spacing distribution is given by the Gaussian orthogonal random matrix ensemble. Our data allow us to see the difference to the Wigner surmise. In particular, our result differs from the critical level-spacing distribution observed at the metal-insulator transition in the three-dimensional Anderson model of disorder.

PACS numbers: 71.23.Ft, 71.30.+h, 05.45.+b, 72.15.Rn

Following the pioneering works of Wigner and Dyson [1], random matrix theory (RMT) has been successfully applied to investigate a great variety of complex systems such as nuclear spectra, large atoms, mesoscopic solids, and chaotic quantum billiards [2–5]. In such systems, it has been shown that spectral fluctuations can be modeled by universal level-spacing distributions (LSD) such as, e.g., $P_{\rm GOE}(s)$ for the Gaussian orthogonal random matrix ensemble (GOE) [2].

A natural application of RMT concerns disordered systems [6]. It has been shown that the metal-insulator transition (MIT) in the three-dimensional (3D) Anderson model of localization is accompanied by a transition of the LSD $P(s)$ [7–9]. Here, s denotes the energy spacing in units of the mean level spacing Δ. In the metallic regime, $P(s)$ closely follows the Wigner surmise $P_{\rm W}(s) = \pi s \exp(-\pi s^2/4)/2$, which is a good approximation of $P_{\rm GOE}(s)$ for which no closed formula is known [2]. On the insulating side, $P(s)$ is given by Poisson's law $P_{\rm P}(s) = \exp(-s)$. One important difference between the two distributions is their small-s behavior [2]: $P_{\rm GOE}(s \to 0) \approx 1.645\, s$ and $P_{\rm P}(s \to 0) \approx 1$, indicating level repulsion and clustering, respectively. At the MIT, where the eigenstates are multifractal [10], another LSD, $P_c(s)$, has been observed [7–9].

Multifractal eigenstates — neither extended nor exponentially localized — have also been found in tight-binding (TB) models of quasicrystals. In fact, these seem predominant in 1D and 2D [11]; in 3D, the attainable system sizes are yet too small for definite statements [12]. The multifractality is assumed to be connected to the unusual transport properties of quasicrystals [13], e.g., their resistivity increases considerably with decreasing temperature and improving structural quality of the sample. Thus, one may speculate that the LSD in quasiperiodic models is also distinct from $P_{\rm GOE}(s)$ and $P_{\rm P}(s)$.

Quasicrystals lack the translational symmetry of periodic crystals, but still retain long-range (orientational) order and show non-crystallographic symmetries incompatible with lattice periodicity. Thus, they constitute a class of materials somewhere in between perfect crystals and amorphous systems. Besides quasicrystals with icosahedral symmetry [14], which are aperiodic in any direction of the 3D space, also dodecagonal [15], decagonal

[16], and octagonal [17] phases have been found, which can be viewed as periodic stacks of quasiperiodic planes with 12-, 10-, and 8-fold symmetry, respectively. Structure models of quasicrystals are based on quasiperiodic tilings which can be constructed, e.g., by projection from higher-dimensional periodic lattices [18]. We emphasize that such quasiperiodic tilings, albeit yielding perfect rotationally symmetric diffraction patterns, exhibit n-fold rotational symmetry in a generalized sense only. In particular, there need not be a point with respect to which the tiling has an *exact* global n-fold rotational symmetry. If such a point exists, it is unique.

In order to understand the transport properties of quasicrystals [13], TB models defined on aperiodic tilings (notably the Penrose tiling) have received considerable attention [11,19–25]. For a TB model defined on the octagonal (Ammann-Beenker) tiling [26], the LSD has also been used to classify the spectrum [23–25]. For periodic approximants, level repulsion was observed [23,24], and $P(s)$ was argued to follow a log-normal distribution [24]. However, a calculation for finite patches with an exact 8-fold symmetry yielded level clustering [25].

In this Letter, we show that these somewhat diverging results become comprehensible when one realizes that the tilings of Refs. [23–25] still retain non-trivial symmetries. In order to obtain the underlying universal LSD, one should consider the irreducible subspectra separately, or break the symmetry by, e.g., either choosing patches without symmetry, or imposing suitable boundary shapes as in quantum billiards, or introducing disorder. It is a peculiarity of the standard periodic approximants [23,24] that the rotational symmetry is violated only weakly, e.g., the number of mismatches after a 90° rotation grows linearly in L for patches of size $L \times L$. Even after removing their exact reflection symmetry [24], the LSD may still show remnants of this almost exact symmetry. Taking this into account, we find that generically the underlying LSD of these non-random Hamiltonians is neither $P_{\mathrm{P}}(s)$ [25], nor log-normal [24], nor $P_c(s)$, but rather $P_{\mathrm{GOE}}(s)$.

Let us reconsider [23–25] the octagonal tiling consisting of squares and rhombi with equal edge lengths as in Fig. 1(a). Besides the projection method mentioned above, one may also use the self-similarity of the tiling to construct ever larger patches by successive inflation steps [27]. E.g., the patch in Fig. 1(a) corresponds to two inflation steps of the inner shaded octagon. On this tiling, we define the Hamiltonian $H = \sum_{\langle i,j\rangle} |i\rangle\langle j|$ with free boundary conditions (BC), $|i\rangle$ denotes the Wannier state at vertex i, and $\langle i,j\rangle$ runs over all pairs of vertices connected by an edge of unit length.

We diagonalize the Hamiltonian and study the LSD of the full spectrum. Due to the bipartiteness of the tiling, the energy spectrum is symmetric about $E = 0$. Furthermore, a finite fraction of the states is degenerate at $E = 0$ [19,22–24]. These correspond to confined states [19] limited to certain local environments, do not contribute to the LSD, and we neglect them. In agreement with previous calculations [23], we find that the integrated density of states (IDOS) is very smooth. This is different from 1D quasiperiodic systems which typically have singular continuous spectra [11]. Nevertheless, the IDOS is not strictly linear as required by RMT, so we "unfold" the spectrum by fitting the IDOS to a cubic spline [8] and use $s_i = N_{\rm av}(E_{i+1}) - N_{\rm av}(E_i)$ for the level-spacing at the ith level with $N_{\rm av}$ the smoothed IDOS. We remark that the LSD is not a bulk quantity since Δ^{-1} is proportional to the system size. In what follows, we shall consider instead of $P(s)$ the integrated level-spacing distribution (ILSD) $I(s) = \int_s^\infty P(t)dt$ which is numerically more stable [8,9]. For completeness, we also compute the spectral rigidity $\Delta_3(L)$ defined in [2].

Fig. 2(a) shows $I(s)$ obtained for an octagonal patch with 157369 vertices corresponding to three more inflation steps of Fig. 1(a). At first glance, $I(s)$ seems to be close to the integrated Poisson law $I_{\rm P}(s) \equiv P_{\rm P}(s)$ as in Ref. [25]. However, this patch has the full D_8 symmetry of the regular octagon, hence the Hamiltonian matrix splits into ten blocks according to the irreducible representations of the dihedral group D_8: using the rotational symmetry, one obtains eight blocks, two of which split further under reflection, while the remaining six form three pairs with identical spectra. This gives a total of seven independent subspectra. As with the confined states, we neglected the exact degeneracies induced by symmetry in Fig. 2(a), since they only contribute to $P(0)$.

The ILSD of the seven independent subspectra are shown in Fig. 2(b). We see that there are only very small differences between the seven ILSD, whereas there are slightly larger deviations to the integrated Wigner surmise $I_{\rm W}(s) = \exp(-\pi s^2/4)$. In Fig. 3, we show the small- and large-s behavior in more detail, restricting ourselves to one irreducible sector. We include data for patches of different sizes, corresponding to two, three, four, and five inflation steps of the inner shaded octagon of Fig. 1(a) with 833, 4713, 27137, and 157369 vertices, respectively. The convergence with increasing size is apparent both for small and large s, but the small deviations from $I_{\rm W}(s)$ still persist. We show in the inset of Fig. 3 that our data in fact follow $I_{\rm GOE}(s)$, obtained by expansion for small s [2], much better than the approximate $I_{\rm W}(s)$. Thus, we attribute the small deviations seen in Fig. 2(b) to the difference between $I_{\rm GOE}(s)$ and $I_{\rm W}(s)$.

The ILSD of the complete spectrum shown in Fig. 2(a) is given by the ILSD $I^{(7)}_{\rm GOE}(s)$ of a superposition of 7 independent subspectra, each of which follows $I_{\rm GOE}(s)$. As shown in Fig. 2(a), it is well approximated by $I^{(7)}_{\rm W}(s)$, defined as the integral of the LSD $P^{(k)}_{\rm W}(s) = \frac{d^2}{ds^2}[\mathrm{erfc}(\frac{\sqrt{\pi}}{2}\frac{s}{k})]^k$ of $k=7$ Wigner spectra, with $\mathrm{erfc}(t)$ the complementary error function [2]. For large k, $I^{(k)}_{\rm GOE}(s)$ and $I^{(k)}_{\rm W}(s)$ approach the Poisson law $I_{\rm P}(s)$. This explains why a previous calculation [25] found a Poisson-like distribution. But our data clearly fit $I^{(7)}_{\rm W}(s)$ better than $I_{\rm P}(s)$. We have obtained similar results also for circular patches, for which one has either D_8, or reflection, or no symmetry, depending on the choice of the center. Thus, the LSD is well approximated by $P^{(7)}_{\rm W}(s)$, or $P^{(2)}_{\rm W}(s)$, or $P^{(1)}_{\rm W}(s) \equiv P_{\rm W}(s)$, respectively.

We can also approximate the octagonal tiling by patches without any exact symmetries. In Fig. 1(b) we show such a square-shaped patch cut out of the octagonal tiling. Although the quasiperiodic 8-fold order is restored in the infinite patch, there is never any exact symmetry present in the finite approximants. The LSD is of the GOE-type as shown in Fig. 2(c) for patches with side lengths $L = 40$, 60, and 80, corresponding to 1980, 4392, and 7785 vertices, respectively. Thus, contrary to the case of a simple square lattice exhibiting level clustering, we find level repulsion. Small deviations from $I_{\rm W}(s)$ are explained as previously using $I_{\rm GOE}(s)$. If one uses square-shaped approximants with symmetries, for instance the D_4-symmetric patch indicated in Fig. 1(a), the LSD is again given by the superposition of the irreducible subspectra. For the standard periodic approximants [23,24], one finds an ILSD between $I_{\rm GOE}(s)$ and $I^{(2)}_{\rm GOE}(s)$ due to the almost exact symmetry mentioned above. Thus, approaching the infinite tiling by square-shaped patches only slightly shifted with respect to each other may give quite different LSD. We have checked that the results are the same for free and periodic BC, e.g., the ILSD for the 5 subspectra of the D_4-symmetric square with 94642 vertices and periodic BC is also close to $I_{\rm GOE}(s)$ as shown in Fig. 2(d), but the finite-size corrections are slightly larger than for free BC.

Choosing patches with special boundary shapes is a different way of excluding symmetries. In fact, this is well known in the context of quantum billiards where it has been used to construct quantum chaotic motion [4,5]. One of the most prominent examples is the Sinai billiard [4,5], which consists of 1/8 of a square and a circular arc centered in the midpoint of the square. Due to these BC, the LSD follows the Wigner surmise even for free electrons [4] instead of a Poisson law which is found for integrable motion in simple square or circular billiards [2]. In Fig. 1(c), we show a Sinai billiard-shaped cut of the octagonal tiling. Moving Sinai's billiard table across the octagonal tiling, we can generate many different patches. However, in contrast to the square-shaped boundary, we never find a case that retains any of the D_8 symmetries. We computed $I(s)$ for quasiperiodic billiards with $L = 70$, 80, 90, 100, and 110, corresponding to patches with 2416, 3146, 3969, 4892, and 5905 vertices, respectively. The results presented in Fig. 2(e) follow $I_{\rm W}(s)$, and, again, are even closer to $I_{\rm GOE}(s)$.

We emphasize that, apart from statistical fluctuations at small and large values of s as shown in Fig. 3, there is no systematic size-dependence of $I(s)$. This is in contrast to the 2D Anderson model at weak disorder [28], where a qualitative change towards Poisson-like behavior for larger system sizes is observed, indicating a finite localization length of the eigenstates. The present size-independence of the LSD is compatible with multifractal and extended states.

In conclusion, we have shown that the energy level statistics of TB Hamiltonians defined on the octagonal tiling with different boundary shapes is very well described by RMT. We can even see that our data fit the exact ILSD $I_{\rm GOE}(s)$ better than the integrated Wigner surmise $I_{\rm W}(s)$. This supports the applicability of RMT for such completely deterministic Hamiltonians. Although there is no randomness in these quasiperiodic models, one may view the absence of translational symmetry as a sort of "topological disorder". We clarify previous statements [23–25] elucidating the importance of symmetry of the finite approximants. We find that the universal LSD for irreducible blocks of a symmetric patch, or for patches without any symmetry, is $I_{\rm GOE}(s)$. Besides the octagonal tiling, we have also considered planar 10- and 12-fold quasiperiodic tilings and obtained analogous results. On the basis of these numerical results, we are led to conclude that the statistical properties of energy spectra of 2D quasiperiodic TB models are generically described by the GOE of RMT. In particular, we never find a critical $I_c(s)$, distinct from $I_{\rm GOE}(s)$ and $I_{\rm P}(s)$, as observed at the Anderson MIT [9]. This is somewhat surprising since eigenstates in these quasiperiodic tilings are multifractal similarly to states at the MIT, and we could have expected that this is reflected in the LSD. Instead, we find that the LSD is similar to the LSD on the metallic side of the MIT.

We thank M. Baake and I. K. Zharekeshev for discussions. JXZ is grateful for the kind hospitality in Chemnitz. Support from DFG (UG), SFB393 (RAR), SEdC and the National Natural Science Foundation of China (JXZ) is gratefully acknowledged. We dedicate this work to Hans-Ude Nissen, one of the co-discoverers of quasicrystals, on the occasion of his 65th birthday.

REFERENCES

[1] E. P. Wigner, Proc. Cambridge Philos. Soc. **47**, 790 (1951); F. J. Dyson, J. Math. Phys. **3**, 140 (1962).

[2] M. L. Mehta, *Random Matrices*, 2nd ed. (Academic Press, Boston, 1990); F. Haake, *Quantum Signatures of Chaos*, 2nd ed. (Springer, Berlin, 1992).

[3] K. B. Efetov, Adv. Phys. **32**, 53 (1983).

[4] O. Bohigas, M. J. Giannoni, and C. Schmit, Phys. Rev. Lett. **52**, 1 (1984).

[5] G. Casati (ed.), *Chaotic Behavior in Quantum Systems: Theory and Application* (Plenum Press, New York, 1985).

[6] B. L. Alt'shuler and B. I. Shklovskii, Zh. Eksp. Teor. Fiz. **91**, 220 (1986) [Sov. Phys. JETP **64**, 127 (1986)].

[7] B. I. Shklovskii, B. Shapiro, B. R. Sears, P. Lambrianides, and H. B. Shore, Phys. Rev. B **47**, 11487 (1993).

[8] E. Hofstetter and M. Schreiber, Phys. Rev. B **48**, 16979 (1993); **49**, 14726 (1994); Phys. Rev. Lett. **73**, 3137 (1994).

[9] I. K. Zharekeshev and B. Kramer, Phys. Rev. Lett. **79**, 717 (1997).

[10] M. Schreiber and H. Grussbach, Phys. Rev. Lett. **67**, 607 (1991).

[11] T. Fujiwara and H. Tsunetsugu, in: *Quasicrystals: The State of the Art*, eds. D. P. DiVincenzo and P. J. Steinhardt (World Scientific, Singapore, 1991), pp. 343–360.

[12] T. Rieth, U. Grimm, and M. Schreiber, in *Quasicrystals: Proceedings of the 6th Int. Conference*, eds. S. Takeuchi and T. Fujiwara (World Scientific, Singapore, 1998).

[13] D. Mayou, in: *Lectures on Quasicrystals*, eds. F. Hippert and D. Gratias (Les Editions de Physique, Les Ulis, 1994), pp. 417–462; C. Berger, *ibid.*, pp. 463–504.

[14] D. Shechtman, I. Blech, D. Gratias, and J. W. Cahn, Phys. Rev. Lett. **53**, 1951 (1984).

[15] T. Ishimasa, H.-U. Nissen, and Y. Fukano, Phys. Rev. Lett. **55**, 511 (1985).

[16] L. Bendersky, Phys. Rev. Lett. **55**, 1461 (1985).

[17] N. Wang, H. Chen, and K. H. Kuo, Phys. Rev. Lett. **59**, 1010 (1987).

[18] C. Janot, *Quasicrystals: A Primer*, 2nd ed. (Clarendon Press, Oxford, 1994).

[19] M. Kohmoto and B. Sutherland, Phy. Rev. Lett. **56**, 2740 (1986); M. Arai, T. Tokihiro, M. Kohmoto, and T. Fujiwara, Phys. Rev. B **37**, 2797 (1988); T. Rieth and M. Schreiber, Phys. Rev. B **51**, 15827 (1995).

[20] Y. Liu and P. Ma, Phys. Rev. B **43**, 1378 (1991).

[21] C. Sire and J. Bellissard, Europhys. Lett. **11**, 439 (1990); J. X. Zhong and R. Mosseri, J. Phys. (France) I **4**, 1513 (1994).

[22] B. Passaro, C. Sire, and V. G. Benza, Phys. Rev. B **46**, 13751 (1992).

[23] V. G. Benza and C. Sire, Phys. Rev. B **44**, 10343 (1991).

[24] F. Piéchon and A. Jagannathan, Phys. Rev. B **51**, 179 (1995); —, private communication.

[25] J. X. Zhong and H. Q. Yuan, in *Quasicrystals: Proceedings of the 6th Int. Conference*, eds. S. Takeuchi and T. Fujiwara (World Scientific, Singapore, 1998).

[26] R. Ammann, B. Grünbaum, and G. C. Shephard, Discrete Comput. Geom. **8**, 1 (1992); M. Duneau, R. Mosseri, and C. Oguey, J. Phys. A **22**, 4549 (1989).

[27] A. Katz, in: *Beyond Quasicrystals* (Springer, Berlin, 1995), pp. 141–189.

[28] K. Müller, B. Mehlig, F. Milde, and M. Schreiber, Phys. Rev. Lett. **78**, 215 (1997).

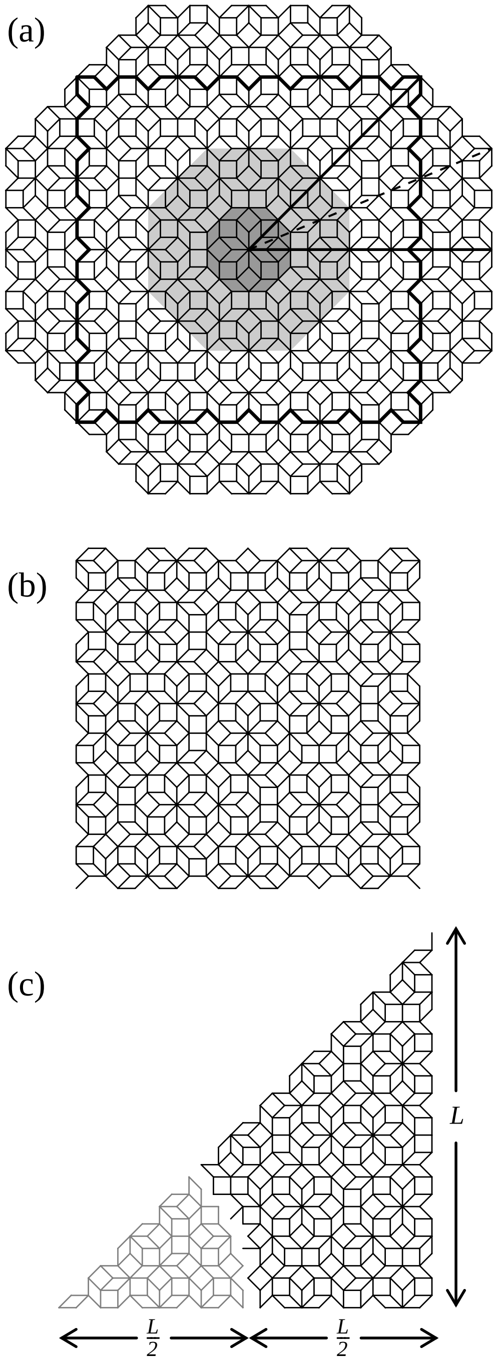
(a)
(b)
(c)
L
L/2
L/2

FIG. 1. (a) Octagonal cluster of the Ammann-Beenker tiling with 833 vertices and exact D_8 symmetry around the central vertex $(x, y) = (0, 0)$ as indicated by the solid and dashed lines. Shadings indicate successive inflation steps of the central octagon. The bold line circumferences a D_4-symmetric cut. (b) Square-shaped cut with 496 vertices defined by $0 \leq x \leq L$, $-\frac{L}{4} \leq y \leq \frac{3L}{4}$ with $L = 20$. (c) Sinai billiard-shaped patch with 246 vertices defined by $0 \leq y \leq x \leq L$ and $x^2 + y^2 \geq \frac{L^2}{4}$ with $L = 22$. Gray edges correspond to the interior of the circular arc; edges crossing the arc are deleted.

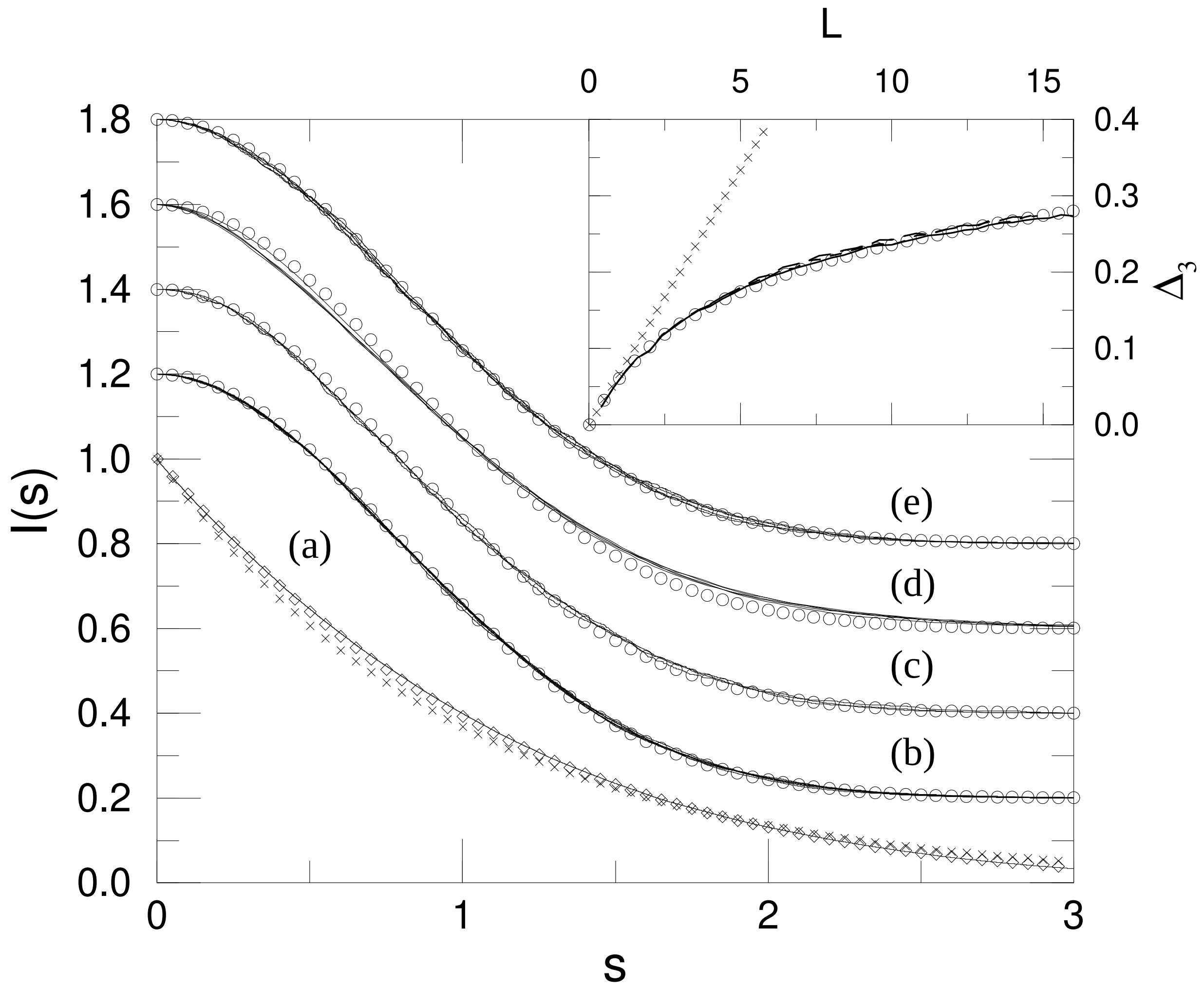

FIG. 2. ILSD $I(s)$ for (a) the largest D_8-symmetric octagonal patch, crosses ($\times$) indicate $I_{\rm P}(s)$, diamonds ($\diamond$) indicate $I_{\rm W}^{(7)}(s)$; (b) the seven independent subspectra of the largest D_8-symmetric octagonal patch; (c) squared-shaped patches of different sizes without internal symmetry; (d) the subspectra of the D_4-symmetric patch with periodic BC; (e) Sinai billiard-shaped patches of different sizes. In (b)–(e), $I(s)$ has been shifted by multiples of 0.2 for clarity, circles ($\circ$) indicate $I_{\rm W}(s)$. Inset: Spectral rigidity $\Delta_3(L)$ corresponding to (b), (c), and (e); $\times$ ($\circ$) indicates Poisson (GOE) behavior.

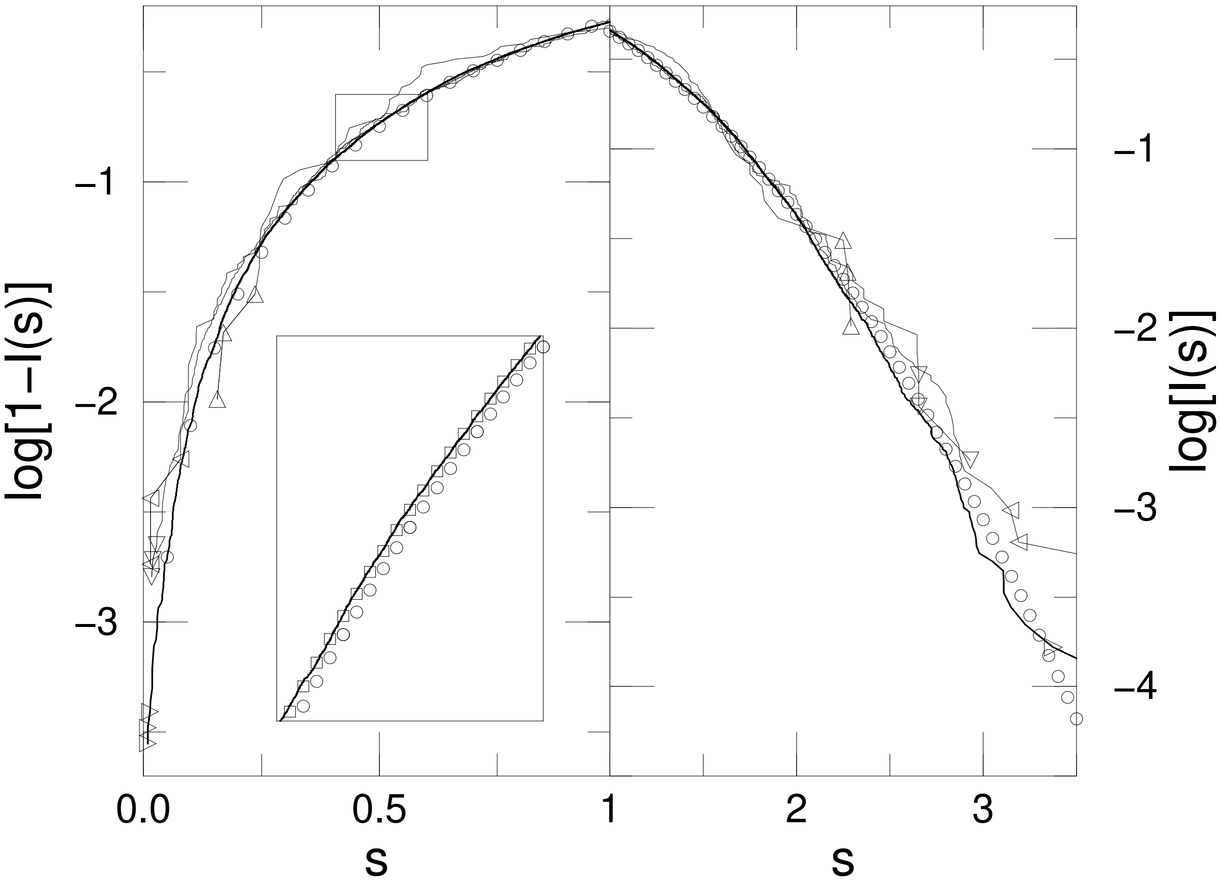

FIG. 3. Small-s (left) and large-s (right) behavior of $I(s)$ for one irreducible sector of D_8-symmetric octagonal patches of different sizes. The bold line corresponds to the largest patch. The three smallest and largest level spacings for each patch are denoted by triangles of different orientations. The circles ($\circ$) indicate $I_{\rm W}(s)$. Inset: Blow-up of the data region enclosed by the rectangle, showing only data for the largest patch. Squares ($\Box$) indicate $I_{\rm GOE}(s)$.